Solid State Ionics 58 (1992) 33–40
North-Holland

SOLID STATE IONICS

Three-electrode current–voltage measurements on erbia stabilized bismuth oxide with co-pressed gold gauze electrodes

I.C. Vinke, B.A. Boukamp [1], K.J. de Vries and A.J. Burggraaf

Laboratory for Inorganic Chemistry, Materials Science and Catalysis, Department of Chemical Technology, University of Twente, P.O. Box 217, 7500 AE Enschede, The Netherlands

Received 28 June 1991; accepted for publication 3 June 1992

The polarization behaviour of $(Bi_2O_3)_{0.75}(Er_2O_3)_{0.25}$(BE25) with a co-pressed gold gauze electrode was studied as a function of temperature and oxygen partial pressure in a three electrode cell. The anodic polarization is smaller than the cathodic polarization. The cathodic charge transfer coefficient, α_c, is about 0.5 while the anodic one, α_a, is about 1.5. The exchange current density shows a $(P_{O_2})^{1/2}$ dependence for partial pressures below 1 atm with an activation enthalpy of $\sim$126 kJ mol^{-1}. These values compare well with results obtained from ^{18}O exchange experiments. Current densities for the co-pressed gold gauze electrodes are about a factor of 5 to 10 larger than found for the previously reported porous sputtered gold electrodes. Analysis of the electrode impedance shows strong influence of surface diffusion on the electrode reaction, which must take place at the surface of the electrolyte.

1. Introduction

A study of the polarization behaviour of $(Bi_2O_3)_{0.75}(Er_2O_3)_{0.25}$(abbreviated BE25) with sputtered porous gold electrodes has been presented by us in a recent paper [1]. A comparison with sputtered, porous platinum electrodes showed that the type of electrode material has little influence on the polarization behaviour. Together with the analysis of both electrode morphologies this led to the conclusion that the surface of the electrolyte must be active in the electrode reaction. For this new concept no theoretical description is yet available.

The analysis was further complicated by a P_{O_2} dependent activation enthalpy for the exchange current density, and a temperature dependent anodic charge transfer coefficient, α_a. This was interpreted as a shift in the type of reaction mechanism going from low to high temperature.

From literature it is known that the electrode morphology can have a large influence on the polarization characteristics of an electrochemical system [2–4] and can strongly influence the reaction mechanism. For the oxygen pumping characteristics of $Bi_{0.571}Pb_{0.428}O_{1.285}$ Dumélié et al. [4] observed an improvement by a factor of five in the performance by using co-pressed gold gauze, instead of vacuum deposited gold, as electrodes. In view of this we decided to use co-pressed gold gauze electrodes in order to obtain a well defined and simple electrode geometry and to improve the electrode/electrolyte contact. The electrochemical data on BE25 with co-pressed gold gauze electrodes are compared with the results obtained for sputtered gold electrodes [1] and changes in the electrode reaction mechanism are evaluated.

2. Experimental

The samples were prepared from the same powder used in the other experiments [1,5]. The working electrode was prepared by cutting an annular ring (outer diameter 10 mm, inner diameter 5 mm) from a gold grid of 1024 mazes mm^{-2} and a wire thickness of 0.06 mm. This ring was placed at the bottom

[1] To whom all correspondence should be addressed.

of a steel die. Enough powder was placed on top of the ring to obtain a disk of more than 1 mm thickness after sintering. The powder was subsequently uni-axially and isostatically pressed and sintered as described previously [5]. After sintering, a sample with a diameter of 12 mm was drilled from the pellet. Care was taken to keep the co-pressed electrode in the centre of the sample.

After sintering the gold gauze was largely buried in the electrolyte material. Samples were therefore ground and polished to expose the gauze to the ambient and to allow contact between the electrode and the electrical contacts in the measurement cell. For the final polish 6 μm diamond paste was used. During the grinding process the electrode morphology was checked with an optical microscope. After obtaining the desired morphology (more then 50% of the gold mesh exposed at the surface) the electrode was polished. The opposite side of the disk was also ground and polished and a counter electrode with the same nominal dimensions as the gauze electrode was applied by dc-sputtering as described previously [6]. The sample was then treated as the samples with sputtered working electrodes [1,6].

3. Results

3.1. Polarization measurements

Fig. 1 shows some typical current–voltage curves measured on BE25 with co-pressed electrodes. These do not deviate markedly from the curves measured on BE25 with sputtered gold electrodes [1]. The currents for the sputtered electrodes are equal within a factor of two compared with the currents of the co-pressed gauze electrode measured on a nominally equal surface.

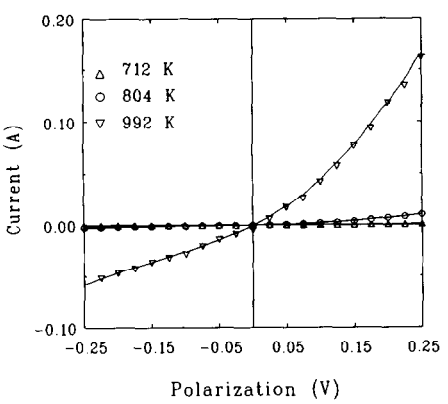

Fig. 1. Typical examples of current–voltage curves for BE25 with co-pressed gold gauze electrodes measured in air.

Differences in the exchange current density, i_0, values are larger due to the difference in α_a values, as shown below. As for BE25 with sputtered electrodes, hysteresis is observed in the polarization curve at lower temperatures. As this hysteresis may influence the polarization parameters significantly, data below 750 K are not considered in the discussion except for the estimation of the exchange current density.

The polarization (I–V) curves could be analyzed in terms of a Butler–Volmer type equation using the NLLS-fit procedure described in refs. [6,7]. In this procedure the non-Faradaic resistance $R_{u(nknown)}$ is also entered as an adjustable parameter (see ref. [1]). The drawn lines in fig. 1 are simulated using the electrochemical parameters obtained from the NLLSF analysis.

In fig. 2 the oxygen exchange current densities are presented as a function of temperature and P_{O_2}. A strong dependence of i_0 on the P_{O_2} is observed. In the temperature region above 725 K the activation enthalpy is independent of the P_{O_2} (with exception

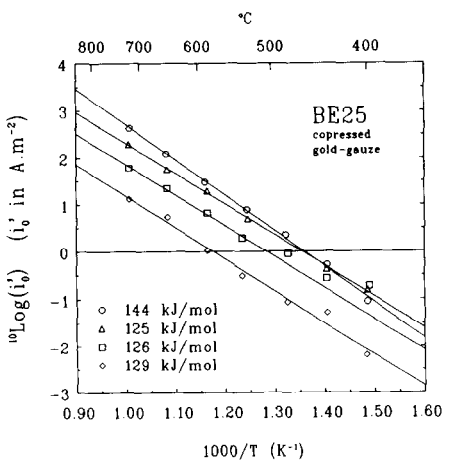

Fig. 2. Oxygen exchange current densities for BE25 with gold gauze electrodes measured at different oxygen partial pressures: P_{O_2} = 1.0 atm (○), 0.21 atm (△), 0.05 atm (□) and 0.001 atm (◇).

of the line for pure oxygen). This is in contrast with results obtained with the sputtered gold electrodes [1]. The activation enthalpy for $P_{O_2}=1.0$ atm ($\Delta H \approx 144$ kJ mol^{-1}) is about 10% larger than those for the other P_{O_2} values ($\Delta H \approx 126$ kJ mol^{-1}). The values for the activation enthalpy for i_0 are reasonably close to the values observed for the sputtered electrodes ($\Delta H \approx 121$ to 157 kJ mol^{-1}) and also close to the value of 130 kJ mol^{-1} observed for the oxygen isotope exchange rates [8]. The activation enthalpies are also in good agreement with the value of 125 kJ mol^{-1} observed by Verkerk et al. [2] for BE20 and BE30 with sputtered platinum electrodes.

For temperatures above 750 K the P_{O_2} and temperature dependence of the i_0 values can be described by:

$$I_0 = k_0 \exp\left(\frac{-\Delta H}{RT}\right) \cdot P_{O_2}^{1/2} . \quad (1)$$

NLLSF-analysis of this data set, excluding the data obtained in pure oxygen ($P_{O_2}=1$ atm), shows a $(P_{O_2})^n$ dependence with $n \approx 0.5$ and an activation enthalpy of ~ 126 kJ mol^{-1}. Similar P_{O_2} dependence was observed for BE25 with sputtered gold electrodes at high temperatures [1] and for erbia stabilized bismuth oxides with sputtered platinum electrodes (Verkerk et al. [2]), also only at high temperatures. Comparison of the i_0 values, fig. 3, shows that the values for co-pressed gold gauze electrodes are 5 to 10 times larger than for sputtered gold electrodes measured under identical conditions (T,P_{O_2}).

The anodic and cathodic charge transfer coefficients are rather constant as shown in fig. 4a. The cathodic charge transfer coefficients, α_c, are close to 0.5 as was observed also for both sputtered Au and Pt electrodes [1]. For the gauze electrodes the anodic charge transfer coefficients, α_a, scatter around 1.5. Hence the sum of the coefficients also scatters around 2 as can be seen in fig. 4b. For the sputtered gold electrodes this is only observed at temperatures above 800–850 K. The small differences between the α-values for co-pressed and sputtered electrodes are,

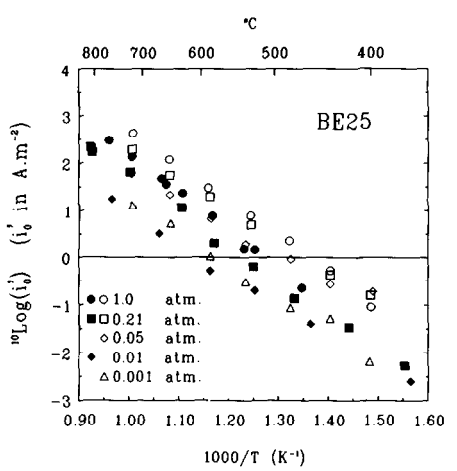

Fig. 3. Comparison of the exchange current density values, i_0, for gold gauze electrodes (open symbols) and for sputtered gold electrodes (closed symbols) taken from ref. [1].

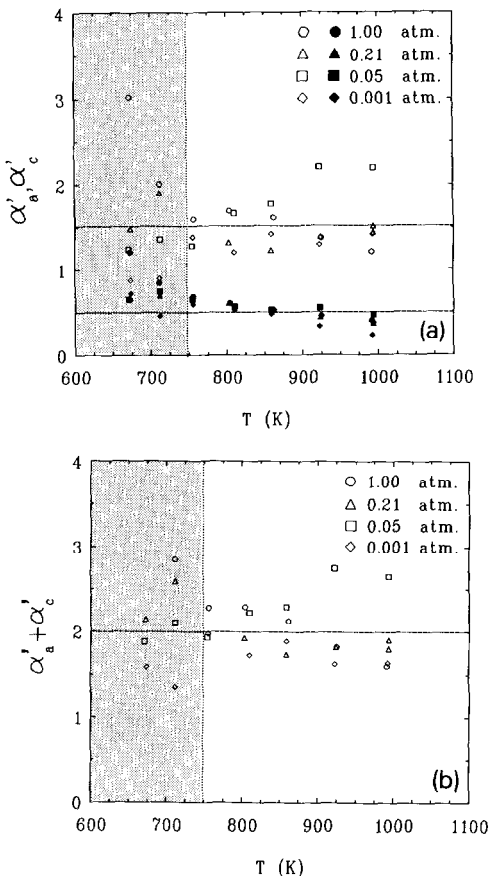

Fig. 4. (a) Anodic (open symbols) and cathodic (closed symbols) charge transfer coefficients for the gold gauze electrodes as a function of temperature and P_{O_2}. (b) Sum of the charge transfer coefficients. The shaded areas indicate the temperature region where hysteresis in the polarization behaviour occurs (see also ref. [1]).

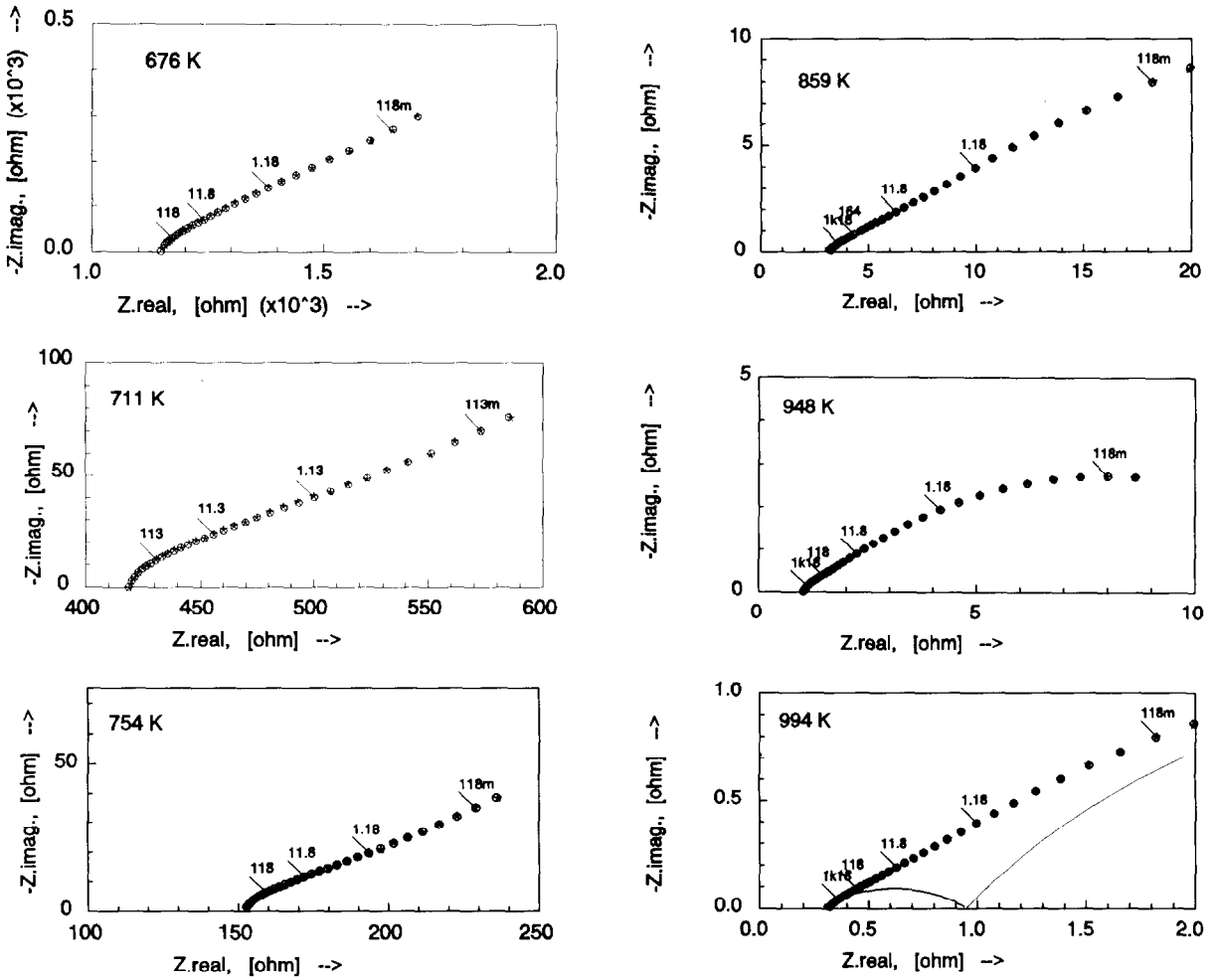

Fig. 5. Impedance diagrams for the BE25/gold gauze electrode measured in air as a function of temperature: ((★) measured data points, (○) results from NLLSF analysis). Frequencies are in Hz. For the measurement at 994 K the drawn line represents the contributions to the dispersion of the separate sub-circuits.

however, responsible for generating differences in electrode currents of only a factor of 2 with a difference in i_0 of a factor of 5 to 10.

3.2. Independence measurements

The Nyquist diagrams of fig. 5 show a few representative impedance spectra for BE25/gold gauze, measured in air. After correcting for the high frequency inductive effect due to the potentiostat, the dispersions were first analyzed with the equivalent

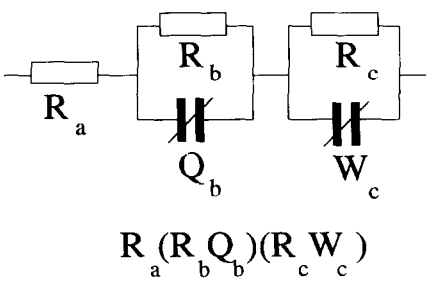

Fig. 6. Schematic representation of the equivalent circuit used in the NLLSF-analysis of the BE25/gold gauze electrode impedance.

Table 1
Parameter values for the equivalent circuit used in the NLLSF-analysis of the electrode impedance of BE25/gold gauze measured in air.

T (K)	R_a (Ω)	R_b (Ω)	Q_b (Ω^{-1} xs^{nb})	n_b	R_c (Ω)	W_c (Ω^{-1} xs$^{1/2}$)
676	1100	1000	1.7×10^{-3}	0.34		5.9×10^{-3}
704	400	260	4.2×10^{-3}	0.31		2.2×10^{-2}
754	140	150	8.8×10^{-3}	0.37		4.4×10^{-2}
803	27	140	1.4×10^{-2}	0.29	750	2.2×10^{-2}
859	2.8	6.6	6.4×10^{-2}	0.33	51	7.3×10^{-2}
948	0.86	0.63	1.1×10^{-1}	0.42	13	8.8×10^{-2}
994	0.28	0.67	6.4×10^{-1}	0.33	5.1	7.4×10^{-1}

circuit used for the sputtered gold electrodes presented in the previous paper [1]: $R_0(R_1Q_1)(R_2Q_2)$. Here the symbolic notation for equivalent circuits described in ref. [9] is used. The NLLSF analysis [9] indicated however, within the limits of the experimental error, a pure Warburg behaviour for the constant phase element Q_2. Hence the element Q_2 was replaced by a Warburg, or semi-infinite diffusion element, W_c as presented in fig. 6. Results of the NLLSF analysis using this equivalent circuit are presented in table 1. Here R_a is equivalent with R_0, the resistance due to the non-Faradaic potential drop between the reference and work electrode.

Elements other then R_a are connected to the electrode process. The sub-circuit (R_cW_c) is assumed to be equivalent to the sub-circuit (R_2Q_2) observed for the sputtered gold electrode. The admittance of a Warburg element (W) is represented by:

$$Y^*_W(\omega) = Y_0\sqrt{j\omega}\,, \tag{2}$$

which is a special form of the admittance of CPE element (Q):

$$Y^*_Q(\omega) = Y_0(j\omega)^n\,, \tag{3}$$

with $n=\frac{1}{2}$. The Y_0 values for W_c are on the average 3 to 4 times larger than the Y_0 values for Q_2 of the sputtered electrode (compare table 1 with table 1 of the previous paper [1]). As the sub-circuit (R_cW_c) contains a Warburg element, it is clearly associated with a diffusion process. The electrochemical process connected with the (R_bQ_b) sub-circuit for co-pressed gauze electrodes should then be compared with the process connected to the (R_1Q_1) sub-circuit for the sputtered electrodes. For the gauze electrodes the values for the exponent of the CPE, n_b, scatter around 0.3. For the constant phase element, Q_1, of the sputtered electrodes the same low values were observed at temperatures above 750 K (ref. [1], table 1).

3.3. Electrode morphology

The important features of the co-pressed gauze electrode are presented in table 2 together with values for the sputtered porous gold electrode [1]. The most significant difference between the two electrodes is a decrease of the three-phase boundary line length by a factor of 14 for the gauze electrode. For

Table 2
Estimated geometrical parameters for the co-pressed and sputtered electrodes.

Electrode type	Three-phase line (m/m^2)	Electrolyte/electrode contact surface (m^2/m^2)	Electrolyte/gas contact surface (m^2/m^2)	Electrode/gas contact surface (m^2/m^2)
sputtered	1.4×10^5	0.83	0.17	0.86
co-pressed	1.0×10^4	0.65	0.65	0.35
ratio s/c	14	1.28	0.26	2.46

the gauze electrode the electrolyte surface area directly exposed to the ambient is about 4 times larger, while the electrode/ambient area is significantly reduced with respect to the sputtered electrode.

4. Discussion

The difference in polarization behaviour for the co-pressed gold gauze electrode and the sputtered porous gold electrode is not very large. Both show rather high exchange current densities with the anodic polarisation being smaller than the cathodic polarisation. The electrode impedances are also quite similar. The difference in electrochemical parameters is characterized by a simple $(P_{O_2})^{1/2}$ dependence for i_0 and a fairly constant α_a (~ 1.5) for the gauze electrode, while the sputtered electrode exhibits for i_0 a $(P_{O_2})^n$ dependence, with n being temperature dependent (changing from $\frac{1}{8}$ to $\frac{1}{2}$ with increasing temperature) and a T and P_{O_2} dependent α_a (ranging from 1.5 to 2–2.5), see [1]. Also the i_0 value for the gauze electrode is about a factor 5–10 larger.

The major difference, however, is found in the respective electrode morphologies. The three-phase boundary length of the gauze electrode is about a factor of 14 smaller than for the sputtered electrode, while the electrolyte surface area exposed to the ambient is about a factor of 4 larger. Again this strongly suggests, as proposed before in the previous paper [1], that the BE25 electrolyte surface is active in the (electrochemical) exchange of oxygen. The observed differences in the i_0 values can be explained to a large extent by the difference in exposed electrolyte surface areas.

In the previous paper [1] two possible reaction schemes were proposed. In the first one it was considered that neutral oxygen species adsorb at the electrolyte surface and diffuse to the three-phase boundary line (which may be an extended zone) where the charge transfer reaction should take place. In contrast to our observations, such a model would lead to smaller polarization currents for the gauze electrode as the three-phase boundary line is smaller and the mean diffusion distance to the three-phase boundary larger for this electrode morphology.

The second model assumes charge transfer to take place at the electrode surface as suggested by the oxygen isotope surface exchange experiments [10]. This requires, however, an electronically conducting surface. In a study on the phase stability of the closely related yttria-stabilized bismuth oxides Kruidhof et al. [11] observed a composition dependent, limited range of nonstoichiometry for oxygen, which implies the presence of electronic defects in these materials. Recently an even more pronounced nonstoichiometry was found for the erbia-stabilized bismuth oxides [12]. Earlier Verkerk and Burggraaf [13] also suggested the existence of electronic surface conductivity, while our recent, preliminary experiments gave similar results [14].

In this perspective it is worthwhile to analyse the electrochemical parameters in terms of the theory of Bockris and Reddy [15], which gives the following relations for the charge transfer coefficients:

$$\alpha_c = \frac{\gamma_c}{\nu} + r\beta, \tag{4a}$$

$$\alpha_a = \frac{\gamma_a}{\nu} + r - r\beta = \frac{n-\gamma_c}{\nu} - r\beta, \tag{4b}$$

$$\alpha_a + \alpha_c = \frac{\dot{n}}{\nu}, \tag{4c}$$

where γ_a is the number of electrons transferred in the reaction steps prior to the rate determining step in the *anodic*, γ_c the number of electrons transferred in the reaction steps taking place before the rate determing step in the *cathodic* reaction, r the number of electrons transferred in the rate determining step, ν the stoichiometric number and n is the total number of electrons transferred in the electrode reaction. β is a symmetry factor.

With $\alpha_a \approx 1.5$ and $\alpha_c \approx 0.5$ three possibilities can be derived, see table 3. The first option in this table ($r=0$) has no physical significance as no reaction

Table 3
Possible values for the Bockris and Reddy model [15] for BE25 with gauze electrodes with $\alpha_a = 1.5$ and $\alpha_c = 0.5$.

r	β	γ_c	γ_a
0	-	1	3
1	0.5	0	2
2	0.25	0	0

scheme can fulfil the proposed conditions. The most straightforward case is the situation in which $r=2$. This points to a charge transfer controlled reaction in which two electrons are transferred simultaneously:

$$O_{ad} + 2e' + V_O^{\cdot\cdot} \rightleftarrows O_O^{\times} \,. \qquad (5)$$

This charge transfer reaction is the basis of the model proposed by Robertson and Michaels [16], who assume this reaction to take place in the zone between the metal electrode and the electrolyte. The simultaneous participation of two electrons in one reaction step on a non-metallic surface, as in the case presented here, would be less likely. Hence this reaction scheme does not seem very probable.

The situation for $r=1$ is more complex. The rate determining step is a one electron transfer reaction which has to be performed twice to complete the overall reaction. After the rate determining step in the cathodic reaction, two more electrons will be transferred. A possible reaction mechanism is:

$$O_2(g) + 2S_{ads} \rightleftarrows 2O_{ad} \,, \qquad (6a)$$

$$2\times\{O_{ad} + e^- \rightarrow O_{ad}^-\} \quad (RDS) \,, \qquad (6b)$$

$$2\times\{O_{ad}^- + e^- + V_O^{\cdot\cdot} \rightleftarrows O_O^{\times} + S_{ads}\} \,, \qquad (6c)$$

where S_{ads} is a surface adsorption site. This model compares well with the suggestion that the formation of O_{ad}^- species is the rate determining step in the surface oxygen exchange reaction [10]. Associative adsorption with one electron transfer followed by dissociation with one electron transfer also leads to the formation of O_{ad}^-. On basis of the Bockris and Reddy theory, however, this scheme does not lead to the α values observed.

Under polarization, gradients in the concentration of the electronic (surface) defects will arrise, extending from the three-phase boundary outwards across the bare electrolyte surface. The electronic defects will be charged (or neutralized) at the noble metal electrode, the resulting gradient will be balanced by a reverse gradient in the occupation of O_{ad}^- across the surface so that electro-neutrality is conserved. Hence diffusion will play an important role in this (qualitative) model. The analysis of the impedance spectra also indicates two diffusional processes, one semi-infinite diffusion type (Warburg) and a CPE-type with a $(\omega)^n$ dependence with $n \approx 0.3$. This CPE behaviour may be due to surface roughness, although other distribution models may apply.

For zero polarization a mass transport free exchange current density will be observed, which should be comparable to the ^{18}O exchange rate, k_s, determined from exchange experiments. A comparison based on the relation $i_0 = 4\,F\,k_s$ is presented in fig. 7. The activation enthalpies for i_0 for the gauze electrode and for k_s are almost equal (126 kJ mol^{-1} versus 130 kJ mol^{-1}). Why i_0 is about a factor 2 higher than the value calculated with k_s is not clear.

As transport through or across the electrolyte surface towards and from the electrode is involved, the mesh size of the gauze used may be an important factor. Above a certain maze width (in the order of the "surface diffusion" length) the electrode current will be a function of the maze size.

The suggested mechanism of eq. (6), based on the theory of Bockris and Reddy, leads to a model that incorporates a number of properties observed for the BE25/co-pressed gold-gauze electrode system:

(i) Indifference for the electrode material used as adsorption and charge transfer takes place at the electrolyte surface.

(ii) Adsorption of oxygen is dissociative.

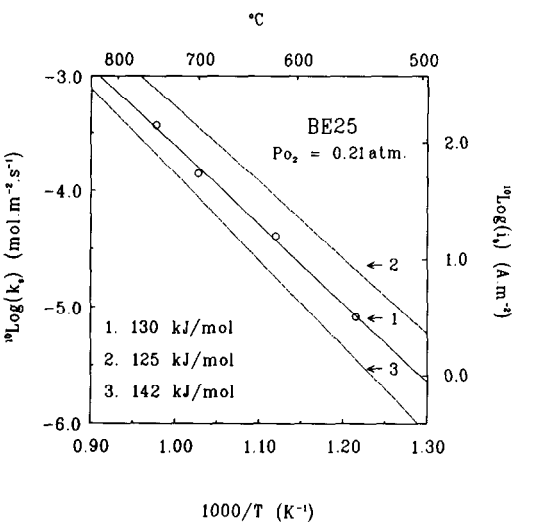

Fig. 7. Comparison of the surface oxygen exchange rate k_s (1, left vertical axis), established from isotope exchange experiments [10], with the exchange current densities (right vertical axis) for BE25/gold gauze (2) and BE25/gold sputtered electrodes (3).

(iii) Diffusion plays an important role in the electrode reaction.
(iv) The surface must be electronically (hence mixed-) conducting.
(v) The values for the charge transfer coefficients can be explained.

The important difference of this (qualitative) model with respect to the diffusion limitation models of Wang and Nowick [17] and of Robertson and Michaels [16] is that the electron concentration is not fixed as in a metal electrode, but varies across the electrode, while the occupation degree of the O_{ad}^{-} species not only depends on the diffusion rate and the charge transfer rate, but also on the adsorption/desorption and dissociation rate of the ambient oxygen. Further research will be needed to derive a mathematical model that will describe the polarization behaviour and the electrode impedance more quantitatively.

5. Conclusions

The electrode behaviour for co-pressed gold gauze electrodes and sputtered gold electrodes on BE25 is comparable.

The oxygen exchange current density for BE25 with co-pressed gold gauze electrodes is 5 to 10 times higher than for BE25 with sputtered gold electrodes and the activation enthalpy is independent of P_{O_2} in the pressure range 0.21 atm to 0.001 atm.

The *entire* surface of the electrolyte is active in the oxygen exchange reaction.

Diffusion plays an important role in the electrode reaction mechanism.

Acknowledgement

The research presented in this paper was supported by the Netherlands Foundation for Chemical Research (SON) with financial aid from the Netherlands Organisation for Scientific Research (NWO).

References

[1] I.C. Vinke, B.A. Boukamp, K.J. de Vries and A.J. Burggraaf, Solid State Ionics 51 (1992) 249.
[2] M.J. Verkerk, M.W. Hammink and A.J. Burggraaf, J. Electrochem. Soc. 130 (1983) 70.
[3] S.P.S. Badwal and F.T. Ciacchi, Solid State Ionics 18/19 (1986) 1054.
[4] M. Dumélié, G. Nowogrocki and J.C. Boivin, Solid State Ionics 28–30 (1988) 524.
[5] H. Kruidhof, K. Seshan, B.C. Lippens Jr., P.J. Gellings and A.J. Burggraaf, Mat. Res. Bull. 22 (1987) 1635.
[6] I.C. Vinke, K. Seshan, B.A. Boukamp, K.J. de Vries and A.J. Burggraaf, Solid State Ionics 34 (1989) 235.
[7] B.A. Boukamp, I.C. Vinke, K. Seshan, K.J. de Vries and A.J. Burggraaf, Solid State Ionics 28–30 (1988) 1187.
[8] B.A. Boukamp, I.C. Vinke, K.J. de Vries and A.J. Burggraaf, Solid State Ionics 32/33 (1989) 918.
[9] B.A. Boukamp, Solid State Ionics 20 (1986) 31.
[10] I.C. Vinke, Electrochemical and electrode properties of stabilized bismuth-oxide ceramics, Ph.D. Thesis (University of Twente, the Netherlands, 1991) Ch. 7
[11] H. Kruidhof, K.J. de Vries and A.J. Burggraaf, Solid State Ionics 37 (1991) 213.
[12] H. Kruidhof, H.J.M. Bouwmeester, K.J. de Vries, P.J. Gellings and A.J. Burggraaf, Solid State Ionics 50 (1992) 181.
[13] M.J. Verkerk and A.J. Burggraaf, J. Electrochem. Soc. 130 (1983) 78.
[14] I.C. Vinke, Electrochemical and electrode properties of stabilized bismuth-oxide ceramics, Ph.D. Thesis (University of Twente, the Netherlands, 1991) Ch. 6.
[15] J.O.M. Bockris and A.K.N. Reddy, Modern Electrochemistry, Vol. 2 (Plenum Press, New York, 1970) Ch. 9.
[16] N.L. Robertson and J.N. Michaels, AIChE (Symp. Ser. 254) 83 (1987) 56.
[17] D.Y. Wang and A.S. Nowick, J. Electrochem. Soc. 128 (1981) 55.